This is an emulation of *Solar Physics* **?** 1 – 18, 2009
The authoritative version is DOI: 10.1007/s11207- ?

Why Temperature and Velocity have Different Relationships in the Solar Wind and in Interplanetary Coronal Mass Ejections?

P. Démoulin

Received 19 November 2008; accepted 20 march 2009

Abstract *In-situ* observations of the solar wind (SW) show temperature increasing with the wind speed, while such dependence is not observed in interplanetary coronal mass ejections (ICMEs). The aim of this paper is to understand the main origin of this correlation in the SW and its absence in ICMEs. For that purpose both the internal-energy and momentum equations are solved analytically with various approximations. The internal-energy equation does not provide a strong link between temperature and velocity, but the momentum equation does. Indeed, the observed correlation in the open magnetic-field configuration of the SW is the result of its acceleration and heating close to the Sun. In contrast, the magnetic configuration of ICMEs is closed, and moreover the momentum equation is dominated by magnetic forces. It implies no significant correlation between temperature and velocity, as observed.

Keywords: Coronal Mass Ejections, Interplanetary; Magnetic fields, Interplanetary; Solar Wind; Velocity Fields, Solar Wind

1. Introduction

Since the pioneering work on the solar wind (SW) in the 1950s and 1960s, especially the seminal work of Parker (1958, 1963), a large number of works and progress in understanding the SW have been made (see *e.g.* Velli, 2001; Cranmer, 2002; Parker, 2007). Still some basic questions remains. For example, what is the dominant mechanism which heats and accelerates the SW? Is it by the cascade of energy to small scale with the development of MHD turbulence, or by the damping of waves (such as Alfvén or ion-cyclotron waves), or is no extra energy input needed, but fast electrons, in the tail of the distribution function, are driving the wind by creating a large scale electrostatic electric field such as in exospheric models? This list of plausible processes is indeed far from exhaustive (see *e.g.* Meyer-Vernet, 2007), showing that the acceleration of the SW is far from being understood.

Observatoire de Paris, LESIA, UMR 8109 (CNRS), F-92195
Meudon Principal Cedex, France
(e-mail: pascal.demoulin@obspm.fr)

An observational clue on the physical processes involved is provided by the *in-situ* measured temperature and its radial gradient away from the Sun. Various spacecraft have accumulated data over a range of solar distances. Only in rare cases two spacecraft are well co-aligned radially to study the evolution of similar plasma blobs with distance (Phillips *et al.*, , 1995; Skoug *et al.*, , 2000). In general, data from only one spacecraft are available. These data do not permit to follow the evolution of plasma blobs as they travel away from the Sun, but they rather provide a statistical result, over a large amount of data, on how the mean plasma temperature changes with distance. This is expected to represent the typical evolution of a blob of plasma traveling outward, so finally this provides a clue as to how much the plasma needs to be heated. The measured temperature (T) is typically fitted with a power law of the distance (r) to the Sun: $T \propto r^{-n_{\rm T}}$ (see references below).

For electron temperature, the results have been summarized by Maksimovic, Gary, and Skoug (2000) in their Table 1. The results are typically in between the isothermal ($n_{\rm T} = 0$) and the adiabatic case ($n_{\rm T} = 1.33$). They range between $n_{\rm T} \approx 0.2$ to 1 between 0.3 and 1 AU (Marsch *et al.*, , 1989; Pilipp *et al.*, , 1990). At larger, distances, typically between 1 and 5 AU, $n_{\rm T}$ is found around 0.8 (Maksimovic, Gary, and Skoug, 2000; Skoug *et al.*, , 2000). When the measurements are restricted to the core of the electron distribution, the results are more spread: $0.4 < n_{\rm T} < 1.1$ between 1 and 5 AU (*e.g.* Issautier *et al.*, , 1998; Skoug *et al.*, , 2000). In fact, the results are difficult to precisely intercompare since they depend on many factors and several of them are typically different between two studies. These include the heliospheric range explored (radial and latitudinal), the binning or not with the SW velocity, the phase of the solar cycle, the part of the electron distribution measured (*e.g.* core, halo, or full distribution), and the criteria used to select the SW period studied. This last point is especially important since the SW contain shocks and interplanetary coronal mass ejections (ICMEs) which are expected to have different thermodynamic properties than the SW.

Inside the inner heliosphere ($r < 1$ AU), the proton temperature is typically decreasing faster with distance than the electron temperature, so the evolution of the protons is more adiabatic (Marsch *et al.*, , 1989; Totten, Freeman, and Arya, 1995). For the range of distance $[1.5, 3.]$ AU, Goldstein *et al.*, (1996) found $n_{\rm T} \approx 1.03$ and ≈ 0.81 for the northern and southern hemisphere, respectively. For the range of distance $[1.5, 4.8]$ AU Feldman *et al.*, (1998) found a proton-temperature evolution close to adiabatic ($n_{\rm T} \approx 1.2 \pm 0.2$). As the interval of distances considered extends further out to 20–40 AU, the proton temperature decrease more similarly to the electron temperature: $n_{\rm T}$ is typically in the interval $[0.5, 0.8]$ (Gazis *et al.*, , 1994; Richardson *et al.*, , 1995; Gazis *et al.*, , 2006). A precise comparison between proton and electron temperatures is however not available since the various authors considered various data sets, in particular different range of solar distances.

Since decades, *in-situ* measurements by spacecraft have shown a clear correlation in the SW between the outward velocity (v) and the proton temperature (T). Lopez and Freeman (1986) fitted several functions $T(v)$ to the SW data. They concluded that the best fit is obtained with T having a quadratic (or cubic) dependance on v for $v < 500$ km s^{-1}, and a linear dependance for $v > 500$ km s^{-1}. Neugebauer *et al.*, (2003) rather used a quadratic function in both v regions, and globally, they found a nearly linear relationship (see their Figure 4). More recently, Elliott *et al.*, (2005) removed the interplanetary coronal mass ejections (ICMEs) from the SW data, and found a different linear law for the compression and rarefaction regions since the SW temperature is systematically lower in rarefaction regions. They also found no evidence for a separate law in the slow and fast wind (as present in previous studies).

Lopez and Freeman (1986) and Totten, Freeman, and Arya (1995) interpreted the $T(v)$ correlation with the variation of the estimated polytropic index within different range of the measured SW velocity. Only recently, Matthaeus, Elliott, and McComas (2006) proposed a theoretical mechanism to explain this correlation. One main purpose of present paper is to further analyze the physics of this $T(v)$ correlation.

Indeed, the observed $T(v)$ correlation is such a strong result that it is recurrently used to define the expected temperature from the measured bulk velocity. When the measured temperature is lower than half the expected temperature, this defines one criteria to identify ICMEs (Richardson and Cane, 1995). ICMEs are formed by the ejection from the Sun of magnetized plasma during CMEs (*e.g.* Wimmer-Schweingruber *et al.*, , 2006; Zurbuchen and Richardson, 2006). Magnetic clouds (MCs) are a particular subset of ICMEs which have a well structured magnetic field; they are formed by twisted magnetic flux tubes, called flux ropes. Though there is still no consensus, non-MC ICMEs are probably also formed by magnetic structures very similar to MCs. It is plausible that MCs are only observed when the spacecraft crosses the magnetic structure close to its centre (Jian *et al.*, 2006) and when the flux rope is not strongly perturbed, for example by an overtaken fast SW stream or by a another MC (see *e.g.* Dasso *et al.*, , 2009 for an example of two interacting MCs forming an extended ICME). Typical characteristics of MCs are partially present in ICMEs, but usually they are less pronounced. This is the case, for example of a lower proton temperature than the expected one in the SW with similar speed. This is also the case for bi-streaming electrons, which are interpreted as flowing along field lines still connected to the Sun. The magnetic configuration of a MC is basically a twisted magnetic field which stay rooted to the Sun, at least partially, for days, if not weeks (*e.g.* Crooker and Horbury, 2006; Attrill *et al.*, , 2008).

The main objective of the present paper is to understand the physical origin of the $T(v)$ correlation in the SW with a simple one fluid model. Then, the internal-energy equation of the plasma is analyzed in Section 2. The heating by MHD turbulence provides a heating which depends on the time spent from the SW launch from the Sun. This type of heating implies a positive $T(v)$ correlation. However, a quantitative comparison of the model to the data shows that T is increasing too slowly with v in this approach. In fact, the acceleration phase of the SW should be taken into account, and the integration of the momentum equation, together with the internal-energy equation, does provide generically a $T(v)$ dependence comparable to observations (Section 3). Then, the same approach provides an explanation for the absence of significant dependence of T on v in ICMEs (Section 4). Finally, the conclusions are given in Section 5.

2. Internal-Energy Budget in the SW

2.1. Basic Equations

Following a blob of plasma, of mass $M = \rho V$, with ρ the mass density and V the volume, the equation of the internal energy (E) in a fluid description is

$$\frac{\mathrm{D}E}{\mathrm{D}t} = -p\frac{\mathrm{D}V}{\mathrm{D}t} + M\ Q - V\ \nabla(\mathbf{q})\,, \tag{1}$$

where Q is the heating per unit time and mass, $\mathbf{q}$ is the heat flux per unit surface and time. The internal energy is $E = f\rho k_{\mathrm{B}}TV/(2\mu)$ and the plasma pressure $p = \rho k_{\mathrm{B}}T/\mu$ with f being the number of degree of freedom of the particles, μ their mean mass, T their mean temperature, and k_{B} the Boltzmann's constant.

Let us consider a stationary flow with all variable depending only on the distance (r) to the Sun. The conservation of mass can be expressed as

$$\rho(r)\ v(r)\ A(r) = f_m\,, \tag{2}$$

where v is the plasma radial velocity, f_m is the mass flux (independent of r), and $A(r)$ is the cross section of the flux tube ($\propto r^2$ for spherical geometry). Then, for a stationary flow, Equation (1) simplifies to

$$\frac{f}{2}\frac{\mathrm{d}T}{\mathrm{d}r} - T\frac{\mathrm{d}\ln\rho}{\mathrm{d}r} = \frac{\rho}{T^{f/2-1}}\frac{\mathrm{d}T^{f/2}/\rho}{\mathrm{d}r} = \frac{\mu}{k_{\mathrm{B}}}\left(\frac{Q}{v} - \frac{\mathrm{d}\ q/(\rho v)}{\mathrm{d}r}\right)\,, \tag{3}$$

with $\mathbf{q} = q\hat{\mathbf{r}}$. Without heating sources ($Q = 0$ and $q = 0$), Equation (3) simplifies to the classical adiabatic case: $T^{f/2}/\rho = T^{1/(\gamma-1)}/\rho =$ constant, where $\gamma = (f+2)/f$ is the adiabatic exponent.

2.2. Correlation Between Temperature and Velocity

The internal-energy equation (3), relates the temperature $[T(r)]$ to the radial velocity $[v(r)]$ when the heating input (Q and q) is known. *A priori*, it is a plausible origin of the observed correlation between T and v as suggested by Matthaeus, Elliott, and McComas (2006). Then, only in present section, let us also suppose that the process accelerating the solar wind is not important for the $T(v)$ correlation, so that $v = U$ is independent of r (this is a good approximation for distances larger than ≈ 0.1 AU). Furthermore, let us write the density as a power law of r

$$\rho = \rho_o(r_o/r)^{n_\rho}\,, \tag{4}$$

where ρ_o is the density at the reference distance r_o. Then, Equation (3) may be rewriten as (with $v = U$)

$$\frac{f}{2}\frac{\mathrm{d}T}{\mathrm{d}r} + n_\rho\frac{T}{r} = \frac{\mu}{k_{\mathrm{B}}}\left(\frac{Q}{U} - \frac{\mathrm{d}\ q/(\rho U)}{\mathrm{d}r}\right)\,. \tag{5}$$

With three degrees of freedom per particle, $f = 3$, $\mu = 0.5\ m_P$ (half proton mass), $n_\rho = 2$, and $q = 0$, this equation simplifies to Equation (1) of Matthaeus, Elliott, and McComas (2006).

With U independent of r, the variable $\zeta = r/U$ is approximately measuring the interval of time spent by the plasma since its departure from the Sun, so its "age" (with an origin set for convenience at the Sun centre). Matthaeus, Elliott, and McComas (2006) made the plausible hypothesis that the heating rate is only a function of the SW age, so they suppose $Q(\zeta)$ and $q = 0$, then Equation (5) is rewritten

$$\frac{f}{2}\frac{\mathrm{d}T}{\mathrm{d}\zeta} + n_\rho \frac{T}{\zeta} = \frac{\mu}{k_\mathrm{B}} Q\,, \tag{6}$$

which has the following general solution

$$T(\zeta) = \frac{2\mu}{k_\mathrm{B} f}\zeta^{-2n_\rho/f}\int_{\zeta_o}^{\zeta} Q(\zeta')\zeta'^{2n_\rho/f}\mathrm{d}\zeta' + T_o\left(\frac{\zeta}{\zeta_o}\right)^{-2n_\rho/f}\,, \tag{7}$$

where T_o is the temperature for $\zeta_o = r_o/U$, and r_o is a reference position close to the Sun.

Since the wind has a uniform velocity (U), we have $\zeta/\zeta_o = r/r_o$, so the last term in Equation (7) is function only of r/r_o. So, for $Q = 0$, the temperature is simply a function of the distance r. In contrast to Matthaeus, Elliott, and McComas (2006), the conclusion is that there is no correlation between T and U for an adiabatic evolution, unless there was already a correlation close to the Sun [so $T_o(U)$].

A correlation $T(U)$ can still be created during the wind propagation with a heating of the form $Q(\zeta)$ since the first term in Equation (7) depends also directly on ζ (and not only on the ratio ζ/ζ_o as for the adiabatic term). For a given distance r this implies in general $T(U)$. Let us express this correlation with Q being a power law

$$Q(\zeta) = Q_1 \zeta^{-n_\mathrm{Q}}\,, \tag{8}$$

where Q_1 and n_Q are constants. This power law is justified below by the observed radial dependence of the SW temperature, see the text after Equation (14), while a more general heating function is simply a sum of power laws with different exponents. With Equation (8), Equation (7) can be written

$$T(\zeta) = \frac{2\mu\ Q_1}{k_\mathrm{B}\ f\ (2n_\rho/f + 1 - n_\mathrm{Q})}\left[\zeta^{1-n_\mathrm{Q}} - \left(\frac{\zeta}{\zeta_o}\right)^{-2n_\rho/f}\zeta_o^{1-n_\mathrm{Q}}\right] + T_o\left(\frac{\zeta}{\zeta_o}\right)^{-2n_\rho/f}. \tag{9}$$

Written explicitly as a function of r and U, with $n_\mathrm{A} = 2n_\rho/f$ being the adiabatic exponent of T, we have

$$T(r,U) = \frac{2\mu\ Q_1\ U^{n_\mathrm{Q}-1}}{k_\mathrm{B}\ f\ (n_\mathrm{A} + 1 - n_\mathrm{Q})}\left[r^{1-n_\mathrm{Q}} - \left(\frac{r}{r_o}\right)^{-n_\mathrm{A}} r_o^{1-n_\mathrm{Q}}\right] + T_o\left(\frac{r}{r_o}\right)^{-n_\mathrm{A}}. \tag{10}$$

Indeed, there is a positive correlation between the SW temperature (T) observed at a fixed position (r) and its velocity (U) if $n_{\rm Q} > 1$, so if, for a given U, $T(r)$ decreases with the distance (r) to the Sun, as indeed is observed.

2.3. Typical Magnitudes for the SW

Let us consider the temperature measured at a distance r_1. Equation (10) is simplified and rendered dimensionless by introducing the reference velocity U_1 and temperature $T_{\rm Q}$ defined by

$$T_{\rm Q} = \frac{2\mu \; Q_1 \; (U_1/r_1)^{n_{\rm Q}-1}}{k_{\rm B} \; f \; (n_{\rm A}+1-n_{\rm Q})} \,. \tag{11}$$

Then Equation (10) can be rewritten

$$T(r,U) = T_{\rm Q} \left(\frac{U}{U_1}\right)^{n_{\rm Q}-1} \left[\left(\frac{r}{r_1}\right)^{1-n_{\rm Q}} - \left(\frac{r}{r_o}\right)^{-n_{\rm A}} \left(\frac{r_o}{r_1}\right)^{1-n_{\rm Q}} \right] + T_o \left(\frac{r}{r_o}\right)^{-n_{\rm A}} . \tag{12}$$

Both U_1 and $T_{\rm Q}$ (see below) are typical values for various SW conditions present at $r = r_1$. At the distance r_1, this further simplifies to

$$T(r_1,U) = T_{\rm Q} \left(\frac{U}{U_1}\right)^{n_{\rm Q}-1} - T_{\rm Q} \left(\frac{U}{U_1}\right)^{n_{\rm Q}-1} \left(\frac{r_o}{r_1}\right)^{1-n_{\rm Q}+n_{\rm A}} + T_o \left(\frac{r_o}{r_1}\right)^{n_{\rm A}} . \tag{13}$$

T_o and r_o are the boundary conditions needed for the integration of the internal-energy equation. They are typically set in the corona. However, here the equations were simplified by supposing that the plasma velocity has no significant radial gradient, so the boundary conditions cannot be set too close from the Sun. A plasma density decreasing as $\approx r^{-2}$ beyond $r_o \approx 10 R_\odot$ is observed (Leblanc, Dulk, and Bougeret, 1998), which implies a nearly-constant velocity beyond r_o from Equation (2) and with $A(r) \propto r^2$, so we set $r_o = 0.05$ AU. In fact, we do not need to be precise in the choice of r_o since, as shown below, using this model the plasma temperature at 1 AU is mostly determined by the interplanetary heating and not by the boundary condition in the corona, when the temperature is decreasing significantly slower with distance than in the adiabatic evolution ($T_{\rm adia} \propto r^{-4/3}$).

Between 0.3 and 5 AU, the mean electron and proton temperature varies typically between r^{-1} and $r^{-0.7}$ (see Section 1), then, the adiabatic term in Equation (12) is unable to explain such gradients since $n_{\rm A} \approx 1.3$. Rather, for $r/r_o >> 1$, the temperature profile is dominated by the first term in the right hand side of Equation (12). We deduce the typical range of $n_{\rm Q}$

$$1.7 \leq n_{\rm Q} \leq 2 \,. \tag{14}$$

Indeed, the needed dominance of the heating term to explain the observed mean temperature gradient in most of the SW streams, and the approximate power law observed for $T(r)$ justify the simple form of Q given by Equation (8) as a first-order estimation.

The typical observed temperature at $r_1 = 1$ AU in the SW is $T_1 \approx 2 \times 10^5$ K for $U = U_1 \approx 600$ km s^{-1}, while the coronal temperature $T_o \approx 10^6$K. Since $r_1/r_o \approx 20$ and $n_{\mathrm{A}} \approx 1.3$, the last term in Equation (13) gives $T \approx 2 \times 10^4$ K, a factor of ten times lower than T_1. With $0.3 \leq 1 - n_{\mathrm{Q}} + n_{\mathrm{A}} \leq 0.6$, the second term provides a contribution relative to the first term ranging between 0.16 and 0.4. The contributions of both second and third terms would be even lower if the boundary conditions were set closer to the Sun. Then, T_{Q} represents approximatively the SW temperature at r_1 for $U = U_1$.

The exponent (n_{Q}) could still extend outside the range given by Equation (14) in some extreme cases. For example, this could be the case if the mean temperature were dominated by electrons with a radial variation as low as $r^{-0.2}$ in SW streams with velocities ≈ 500 km s^{-1}as found by Marsch *et al.*, (1989) between 0.3 and 1 AU. The opposite case would be present if the mean temperature is dominated by protons, since they are found to have a nearly adiabatic evolution in slow SW streams between 0.3 and 1 AU (Lopez and Freeman, 1986). With these extremes, n_{Q} is in the extended range: $1.2 \leq n_{\mathrm{Q}} \leq 2.3$. The consequence of this extended range is also investigated below.

2.4. Comparison to Observations

In this section, we compare the prediction of Equation (13) with observed results. Matthaeus, Elliott, and McComas (2006) analyzed *in-situ* data obtained with *Advanced Composition Explorer* (ACE) spacecraft. This is an extension of the previous work of Elliott *et al.*, (2005) over a time period of seven years. They separated the data obtained inside likely ICME from the SW. The three criteria for ICME are: high α to proton density ratio (> 0.08), high O^{7+} to O^{6+} density ratio (> 1), and low proton β (< 0.1). The data points which satisfy the three ICME criteria defined the likely ICMEs. The data points satisfying at least one of the criterion, or taken within one day of satisfying a criterion, define the possible ICMEs. The selection of the possible ICMEs is broad enough that we can be confident that most of the ICMEs have been selected, so that the remaining data are from the SW (called non-ICME).

Since the heating process of the solar wind is still largely disputed (see Section 1), we cannot rely on a model to derive the amount of heating, then presently theory cannot provide an estimation of the coefficient Q_1 and n_{Q} in Equation (8). However, with the hypothesis $Q(\zeta)$, the observed radial gradient of temperature provides an interval of n_{Q}. With the reference velocity set to $U_1 = 600$ km s^{-1}, we explore a range of T_{Q} values in order to cover the observed range of observed T (Figure 1). This implicitly defined the amount of heat needed, so the coefficient Q_1 [Equation (11)].

By setting T_{Q} in the range of observed values, we force the theory to be close to the observations near $U \approx U_1$. Still, there is a significant deviation between the prediction of Equation (13) and the main trend shown by the observations in the SW (Figure 1). Indeed, assuming $Q(\zeta)$, together with the observed approximative power law for $T(r)$, implies strong constraints on the predicted $T(U)$ correlation deduced from the internal-energy equation.

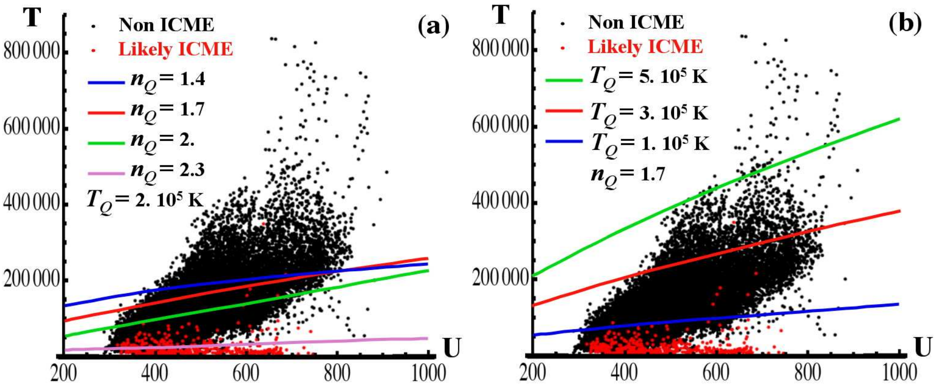

Figure 1. Comparison of the results given by Equation (13) with the results of Matthaeus, Elliott, and McComas (2006). The data points are reproduced from their paper. T is the proton temperature and U is the velocity; both are measured by the ACE spacecraft. The red points are for data which satisfy three ICME criteria (see Section 2.4). A larger set of data points, called "possible ICME", are removed from the measurement series giving the non-ICME data points which are from the SW.

With $n_{\rm Q}$ within the range of Equation (14), the temperature predicted by Equation (13) has a much lower slope than for the SW data (Figure 1a). Extended the range of $n_{\rm Q}$ to lower values simply provides an even lower slope, while increasing $n_{\rm Q}$ does provide a large dependence of T on U for the first term in Equation (13), but as $n_{\rm Q}$ gets closer to $n_{\rm A}+1$, this effect is masked by a larger contribution of the adiabatic term (last term in Equation (13)). Then, increasing $n_{\rm Q}$ to larger values than in Equation (14) does not provide a steeper dependence of T on U (Figure 1a).

Next, modifying the value of T_Q also does not allow to explain the general tendency of the correlation $T(U)$ (Figure 1b). Moreover, as explain above, the boundary values (r_o,T_o) have small influence on these results, so modification of these values also cannot improve the results.

The result of Equation (13) was also compare to the results of Elliott *et al.*, (2005) where they plotted separately the compression and the rarefaction regions (defined by positive and negative slope, respectively, of a 2-day running average of SW speed versus time, and with an absolute slope magnitude above 2.2×10^{-4} km s^{-2}). Even for the best cases ($n_{\rm Q} \approx 1.7$ up to ≈ 2, Equation (13) predicts a too small slope with an intersection of the $T=0$ axis far from $v \approx 250$ km s^{-1} as present in their linear fit of the data (Figure 2), so Equation (13) cannot interpret the mean results of Elliott *et al.*, (2005). Since their linear fit is dominated by the most populated region (the regions in Figures 1 and 2 where individual data points cannot be distinguished), Equation (13) is also not appropriate to interpret the core of the $T(v)$ distribution. Moreover, the increase dispersion of T with increasing v is not explained.

In conclusion, assuming a SW heating that is only a function of $\zeta = r/U$ does provide a positive correlation between T and U in the SW at distances far from the Sun (i.e. where the heating term dominates in the internal-energy equation). But the implied slope in this correlation is significantly lower than observed both

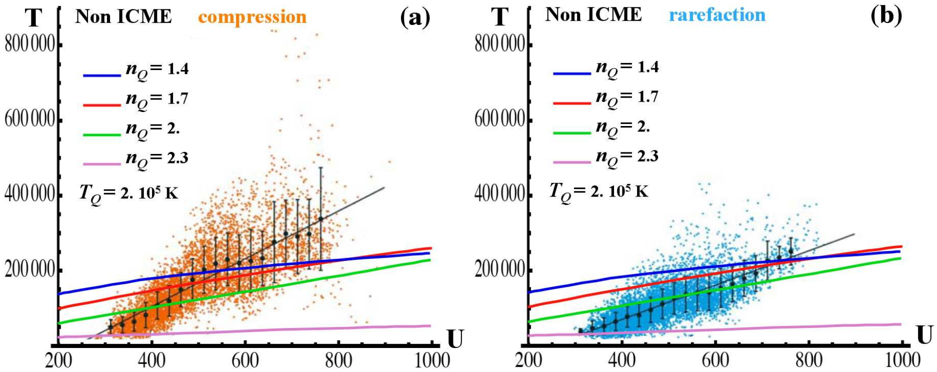

Figure 2. Comparison of the results given by Equation (13) with the results of Elliott *et al.* (2005). The data points are reproduced from their paper. T is the proton temperature and U is the velocity; both are measured by the ACE spacecraft. The orange and blue points are for SW data with compression and rarefaction, respectivelly. The average T, by bins of 25 km s^{-1}, is shown with black dots and the standard deviation with error bars. A linear fit of the binned data is added with a black line.

for the core and the high temperature tail of the distribution (Figures 1, 2). The observed correlation would require a heating term of the form $U^e \zeta^{-n_Q}$ with the exponent e typically in the interval $[2, 3]$. So this would require an *ad hoc* and an important deviation from the concept proposed by Matthaeus, Elliott, and McComas (2006). In the next section, a different approach is explored.

3. Global Energy Budget in the SW

3.1. Correlation Between Temperature and Velocity

The momentum equation is

$$\rho \frac{\mathrm{D}\mathbf{v}}{\mathrm{D}t} = -\nabla p + \mathbf{j} \times \mathbf{B} - \frac{\rho \, G M_{\odot}}{r^2} \hat{\mathbf{r}} + \rho \, \mathbf{f} \, , \tag{15}$$

where $\mathbf{j}$ is the current density, $\mathbf{B}$ the magnetic field, G the gravitational constant, $M_{\odot}$ the solar mass and $\mathbf{f}$ incorporates any extra force per unit mass (*e.g.* deposition of momentum by waves).

For a radially-symmetric and stationary SW flow the radial projection of Equation (15) is

$$v \frac{\mathrm{d}v}{\mathrm{d}r} = -\frac{\mathrm{d}P/\mathrm{d}r}{\rho} - \frac{G M_{\odot}}{r^2} + f_r \, . \tag{16}$$

We have neglected the contribution of the magnetic force since close to the Sun the magnetic field is mainly radial, while at larger distances, when the azimuthal component becomes significant, the magnitude of this force is small compare to the inertial term ($B^2/\mu_0 << \rho v^2$).

The integration of Equation (16) from r_o to r, provides a generalized Bernoulli equation

$$\frac{v^2}{2} + \int_{r_o}^{r} \frac{\mathrm{d}P/\mathrm{d}r}{\rho}\mathrm{d}r - \frac{GM_\odot}{r} - \int_{r_o}^{r} f_r \mathrm{d}r = \frac{v_o^2}{2} - \frac{GM_\odot}{r_o} \,. \quad (17)$$

In contrast to the analysis done in previous section (inside and after Section 2.2), the velocity v is explicitly a function of r. Indeed, as shown below, the increase of v with r, mostly close to the Sun, is the main point giving the correlation between T and v.

The internal-energy equation is provided by Section 2.1. Equations (2,3,17) are coupled equations describing the radial variation of ρ, T, v when boundary conditions are set at r_o. Their numerical solution provides a SW model that depends on the heat input selected (Q,q) and the extra force used (f_r). However, it is also worth simplifying these equations, retaining only the main terms, in order to understand the main physical implications of these equations, in particular for understanding the physical origin of the correlation $T(v)$.

The density in the SW is well described by a power-law (Equation 4), with $n_\rho \approx 2$, since $A(r) \propto r^2$ and $v \approx$ uniform is a good approximation in Equation (2) for $r \geq 0.1$ AU. The temperature is in large measure given by the integration of the internal-energy Equation (3) with only a weak effect on the velocity (Section 2). The velocity is mostly given by the Bernoulli equation. Indeed v increases with r due to the work done by the pressure force. The term $\int_{r_o}^{r} \frac{\mathrm{d}P/\mathrm{d}r}{\rho}\mathrm{d}r$ is approximately proportional to the temperature (with a weighting with the distance within the integral). This is the main origin of the $T(v)$ correlation: with a higher temperature, the wind is accelerated to higher velocity (and most of this acceleration occurs close to the Sun). More precisely, a higher heating rate provides a higher acceleration and a higher temperature. These kinetic and thermal input then propagate to large distance giving a strong $T(v)$ correlation. It implies that the physical base of the correlation is quite general, so that a strong positive $T(v)$ correlation is expected for a large range of models (however exceptions are still possible if the functions Q, q and f_r go strongly against this general behavior of the equations). Below we explore this conclusion with a simple model.

3.2. Example of Correlation with a Polytropic Evolution

In this section we use a particular model to illustrate quantitatively the above deduced $T(v)$ correlation. The model is selected among others to provide analytical results, while being realistic enough to be applied as a first approximation to the SW.

In interplanetary space, the heat flux (q) is expected to be different from the classical value derived for a strongly-collisional plasma since the mean free path of electrons is expected to be comparable or even larger than the typical scale length of the density gradient (especially for electrons above the average thermal energy). In a mostly collision-less plasma, based on previous works,

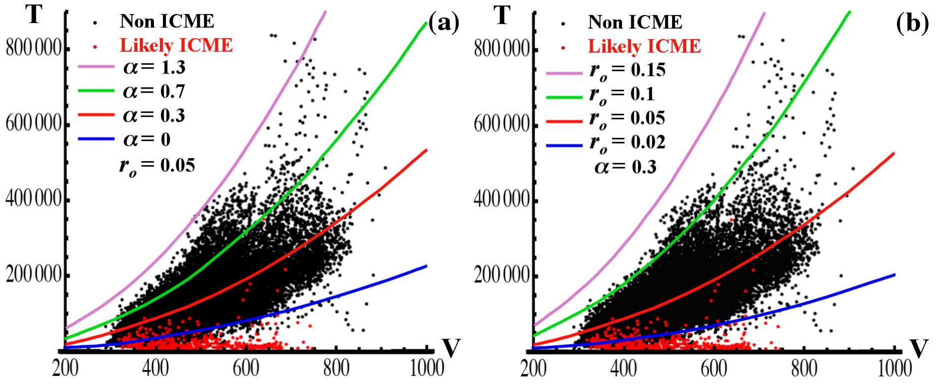

Figure 3. Comparison of the results given by Equation (23) with the results of Matthaeus, Elliott, and McComas (2006). The data points are reproduced from their paper. α is a dimensionless constant defined in Equation (18), and r_o is the distance from the Sun, in AU, where the polytropic law is supposed to begin.

Hollweg (1976) proposed the following expression for the heat flux (see also Meyer-Vernet, 2007 for a recent summary)

$$q = \frac{3\alpha}{2}\frac{\rho}{\mu}\; v\; k_{\mathrm{B}}T\,, \tag{18}$$

where α is a constant of the order of unity and T is the electron temperature (taken here equal to the proton temperature). This approximate expression is derived from an electron distribution function with a tail truncated in the solar direction, and with electrons coupled to protons by an electric field, so that they move globally at the SW speed.

With the above heat flux and $Q = 0$, Equation (3) has an analytical integral giving a polytropic variation of the temperature as a function of the density

$$T = T_o(\rho/\rho_o)^{2/(f+3\alpha)}\,, \tag{19}$$

with a polytropic index $\lambda = 1 + 2/(f + 3\alpha)$. This provides a simple solution of the internal-energy equation, sufficient for the present purpose to derive the $T(v)$ correlation from the momentum equation. This is an extreme case where the temperature is not linked to the velocity in the internal-energy equation.

With Equation (19), the pressure term in Equation (17) is simply integrated

$$\frac{v^2}{2} + (\frac{f}{2} + 1 + \frac{3\alpha}{2})\frac{k_{\mathrm{B}}(T - T_o)}{\mu} - \frac{GM_\odot}{r} - \int_{r_o}^{r} f_r \mathrm{d}r = \frac{v_o^2}{2} - \frac{GM_\odot}{r_o}\,. \tag{20}$$

This is rewritten as

$$\frac{v^2}{2} = (\frac{f}{2} + 1 + \frac{3\alpha}{2})\frac{k_{\mathrm{B}}(T_o - T)}{\mu} + C\,, \tag{21}$$

where C collects all the terms that do not depend on velocity or temperature (here we suppose no such of dependence for f_r to stick to the basic argumentation).

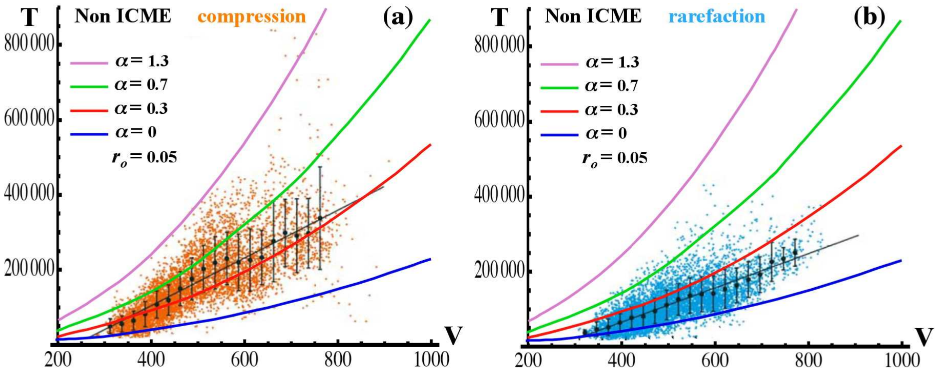

Figure 4. Comparison of the results given by Equation (23) with the results of Elliott *et al.* (2005). The data points are reproduced from their paper. The same curves than in Figure 3a are shown. $\alpha = 0.3$ corresponds to $n_{\rm T} \approx 1$ and $\alpha = 0.7$ to $n_{\rm T} \approx 0.8$ [Equation (22)], so to typical radial temperature gradient observed in the SW.

With Equation (4) and $n_\rho = 2$, Equation (19) may be rewritten as

$$T = T_o (r_o/r)^{4/(f+3\alpha)} \,, \tag{22}$$

so $n_{\rm T} = 4/(f+3\alpha)$. With $n_{\rm T}$ in the range $[0.7, 1]$ and $f = 3$, α is in the range $[0.3, 0.9]$, so of the order of unity as expected by the kinetic theory.

With Equation (22), Equation (21) can be rewritten as

$$T(r,v) = \frac{\mu}{k_{\rm B}} \frac{v^2 - 2C}{f + 2 + 3\alpha} \frac{1}{(r/r_o)^{4/(f+3\alpha)} - 1} \,. \tag{23}$$

For a fixed distance r, and a given heating flux (so α value, or equivalently a given polytropic index λ), the temperature is a quadratic function of the velocity. The comparison to the data is shown in Figure 3 for the simple case $C = 0$, a case where there is not a significant acceleration provided by f_r (just compensating for the difference of gravitation potential). Cases with $C \neq 0$ are simply deduced by translation of the curves along the v-axis when C is not dependent of T and v. If some acceleration model provides such dependence, *via* f_r, then the curves are deformed accordingly.

It is remarkable that such a simple approach provides the main trend present in the observations without inputting extra hypothese. Fixing the parameters, so for a given heat flux (α fixed), for a given range of distances where this heat flux is applicable ($r \geq r_o$), $T(v)$ has a quadratic dependence which is the typical dependence observed if we consider the global distribution of the data points (Figure 3). However, most of the SW data points are grouped in a narrower region (black region). Elliott *et al.*, (2005) found that a linear fit represents well the mean tendency of $T(v)$ for the full range of v, in particular when they split the data between rarefaction and compression regions. Their linear fit are around the curve $\alpha = 0.3$ in Figure 4. It is remarkable that this correspond to a typical value of the temperature gradient in the SW, $n_{\rm T} \approx 1$, independently deduced from other observations (Section 1). This curve (and all the ones in the neighborhood) has indeed a low curvature when restricted to the most dense part of data points. Moreover with the observed dispersion in T this curve can hardly be distinguished from a linear dependance. Then, Equation (23) is also compatible with the mean linear tendency found by Elliott *et al.*, (2005).

The observations show a broad distribution of $T(v)$. Elliott *et al.*, (2005) found a shift in temperature between the rarefaction and compression regions. A broad distribution of $T(v)$ is still present for both data sets, especially for the set of compression regions. This is most likely due to the mixture of SW with different properties, in particular different heating. The above polytropic model also permits to interpret the increase of T dispersion with an increasing v, either from a variable α, either as a variable r_o (Figures 3,4). The physical interpretation is different as follows: a variable α implies a variable efficiency of the heat flux in interplanetary space (probably because of a variable tail in the distribution function of electrons). A variable r_o implies a variable extension of the corona where Equation (18) does not apply (probably because of too many collisions or/and a different distribution function of electrons).

The above results contrast with the results obtained with the internal energy alone (Figures 1,2). The conclusion is that the momentum equation is the main cause of the $T(v)$ correlation. Using the approximation of a velocity spatially uniform, $v = U$, is *a priori* a good approximation for a large part of the heliosphere (except close to the Sun) as shown from both observations and models (for example, with the above model, v is only increasing by 4 to 9% between 0.2 and 1 AU with α in the range $[0, 1.3]$ and $v \approx 600$ km s^{-1}). However, the trick is that applying this approximation from the beginning of the analysis, as done in Section 2 and in Matthaeus, Elliott, and McComas (2006), does not allow us to understand the physical origin of the $T(v)$ correlation.

4. Energy Budget in ICMEs

4.1. Thermal difference between SW and ICMEs

The properties of plasma measured in ICMEs are significantly different than in the SW (see *e.g.* Liu, Richardson, and Belcher, 2005). Moreover, not only is the proton temperature much lower in ICMEs than in the SW, but also the correlation $T(v)$ disappears (or at least is much weaker) as shown by the results of Elliott *et al.*, (2005) and Matthaeus, Elliott, and McComas (2006), reproduced in Figures 1 and 3. Is the heating mechanism different or in a different regime? This is, *a priori*, plausible, in view of the very different characteristics measured in the SW and ICMEs, as follow. In the SW, the magnetic field is variable and the plasma-β fluctuates around unity. In contrast, a well-organized magnetic field with low fluctuations, and a low β (≤ 0.1) are observed in ICMEs (the difference with SW properties is even more pronounced in MCs). However there are no strong observational clues to test this presently.

Three other possibilities, advocated by Matthaeus, Elliott, and McComas (2006), are also, *a priori*, possible, as follows. First, the volume of a parcel of plasma in an ICME is expanding faster than in the SW. Second, ICMEs

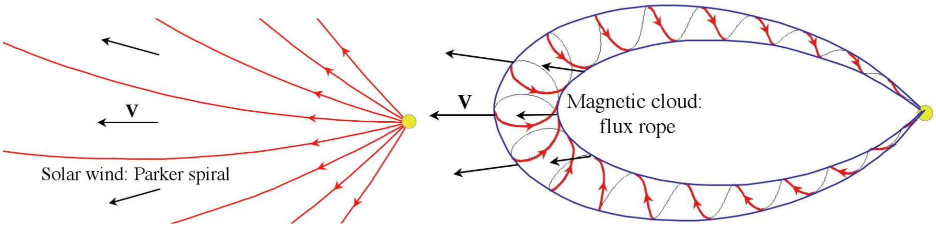

Figure 5. Schematic of the different magnetic field configurations present in the SW and in a flux rope ejected from the Sun (forming a MC or an ICME).

depart from spherical expansion. Finally, the conditions for an heating rate Q depending only on ζ could be absent in ICMEs. Let us analyze these possibilities with the results of Section 2. First, $n_\rho \approx 2$ in Equation (4) for the SW, and $n_\rho \approx 2.3-2.4$ for ICMEs for solar distances larger than 0.3 AU (Liu, Richardson, and Belcher, 2005; Wang, Du, and Richardson, 2005), so ICMEs do expand faster than the SW, but n_ρ is not affecting the dominant term in Equation (12), and more generally in Equation (7), so that the difference in the observed expansion rate between ICMEs and SW cannot explain the strong difference observed for $T(v)$. Closer to the Sun, an important expansion of ICMEs can provide a strong temperature decrease only if the heating term in Equation (7) is not dominant. Next, it is true that ICMEs depart from spherical expansion, but this can be taken into account by $A(r)$ in Equation (2), and in the results of Section 2. This would mainly change n_ρ (Equation 4) with again only a small effect on $T(v)$ as derived from Equations (9-13). Finally, the third proposal above, a fully different heating rate Q, is plausible but it is difficult to test it with observations.

4.2. Expected $T(V)$ relationship in ICMEs

The results of Section 2 show that a heating Q depending only on ζ is not sufficient to explain the observed correlation $T(v)$ in the SW, while including the acceleration of the SW, so solving the momentum equation (15), permits to understand how this $T(v)$ correlation appears (Section 3). The momentum equation is also one of the main equations governing the physics of ICMEs. However, the dominant terms, as well as the geometry of the magnetic field, are different in the SW and in ICMEs, and it is worth analyzing the consequences.

The main difference is that SW magnetic field lines are open, while ICME field lines are closed and still connected to the Sun (at least a majority of them, see Section 1), as sketched in Figure 5. Let us consider different winds with different heating. As the heating increases, the temperature and the plasma pressure increases, accelerating the plasma to higher velocities along the open magnetic field lines. The same happens with a larger deposition of momentum. However, in a closed magnetic configuration, this cannot happen, unless the plasma pressure becomes high enough so that the magnetic configuration is blown up towards an open magnetic-field configuration. In ICMEs, this last case could not happen, since the plasma β is significantly less than unity. A higher heating, or momentum deposition, can only produce a flow along the magnetic field if the deposition is asymmetric between the two legs of the flux rope (*e.g.* this is expected when one leg gets disconnected by reconnection with an open magnetic field). However, this asymmetric input of energy produces at most a flow with a significant radial component (away from the Sun) only if one of the leg of the flux rope is crossed by the spacecraft, but with no coherence in sign between different ICMEs (since both the local heating asymmetry and the observations are expected to be not associated with a specific leg). If rather the leading part of the flux rope is crossed (called the nose), as it is frequently the case for MCs, the extra velocity, produced by the heating or by the momentum deposition, is mostly orthogonal to the radial direction in the core of the flux rope. In conclusion, the results of Section 3 for the SW do not apply to the closed magnetic configuration of ICMEs, and there is no expected correlation between T and v in ICMEs.

Let us summarize further the physics of ICMEs, in order to contrast it with the one present in the SW. The general equation (15) applies to both, but Equation (16) applies only to the SW, since the main term in ICMEs, the Lorentz force, is neglected in Equation (16). Indeed, this magnetic force, together with the contribution of a drag force, determine the temporal evolution of the velocity in ICMEs (Chen, 1989; 1996), in good agreement with the observed velocity of CMEs/ICMEs in the inner heliosphere. Numerical MHD simulations confirm this (*e.g.* Cargill and Schmidt, 2002; Shen *et al.*, , 2007). Even the internal expansion of the flux rope is dominated by the magnetic force, with negligible contribution of the plasma pressure within the flux rope (Démoulin and Dasso, 2009). In summary, the evolution of flux ropes is mainly governed by the balance between their internal magnetic forces and the forces present in the surrounding SW (plasma, magnetic and dynamic pressures, as well as the drag force). Then, the evolution of the field configuration and of the main velocity components (expansion and velocity of the mass centre) of ICMEs, are expected to be nearly independent of the thermodynamics of the ICME plasma. It implies that no significant correlation between T and v is expected in ICMEs, as observed.

5. Conclusion

Since decades, *in-situ* measurements by spacecraft have shown a clear correlation, $T(v)$, in the SW between proton temperature and outward velocity. Lopez and Freeman (1986) had interpreted this correlation with the variation of the estimated polytropic index with velocity. This indicates that a larger energy input is plausibly at the origin of both higher temperature and velocity in the SW.

Only recently, Matthaeus, Elliott, and McComas (2006) proposed a theoretical interpretation for the observed $T(v)$ correlation. They proposed that a specific heating model, MHD turbulence, would provide a heating per unit time and mass which would depend only on the SW age (since its departure from the Sun). Then they showed that the internal-energy equation, with such heating, naturally provides a positive correlation between temperature and velocity, as they observed with the ACE spacecraft at 1 AU. However, after a quantitative analysis, solving the internal-energy equation, the $T(v)$ relation found by this approach has a much weaker dependence on v than that present in observations (Section 2, Figures 1,2).

The previous approach is based on the approximation that the solar wind velocity has negligible radial gradient. This is a good approximation far from the Sun, *e.g.* at distances larger than ≈ 0.1 AU. Still, the magnitude of the SW velocity depends on how it was accelerated, and a theory explaining the $T(v)$ correlation should incorporate explicitly the acceleration region close to the Sun. This implies solving the momentum equation together with the internal-energy equation (Section 3). The link between the acceleration region and the *in-situ* observed region can be realized analytically with an integral form of the momentum equation (giving a generalized Bernoulli's equation). Then, even with an internal-energy equation giving a temperature having no explicit dependence on velocity, Bernoulli's equation provides an *in-situ* temperature depending quadratically on the velocity, basically as observed for the global distribution of the data points (Figures 1,2), while the relation is approximately linear when the data are restricted to the most frequent conditions observed in the SW (Figure 2). In conclusion, the observed $T(v)$ correlation is generically provided by the physics in the acceleration region of the SW: the more it is heated, the faster it blows.

The observations of Elliott *et al.*, (2005) and Matthaeus, Elliott, and McComas (2006) clearly show that the $T(v)$ correlation is not present in ICMEs. With the quantitative results of Section 2 on the internal-energy equation applied to ICMEs, the observed faster expansion rate of ICMEs than in the SW is not at the origin of a different $T(v)$ relation (Section 4). The same conclusion applies to the departure from spherical expansion of ICMEs. Another possibility is that the heating in ICMEs is radically different than in the SW. This is plausible in view of the very different physical conditions present in ICMEs and in the SW, however this needs to be demonstrated. In fact, Section 3 shows that there is a generic cause for a completely different behavior of $T(v)$: the momentum equation is dominated by different terms in ICMEs and in the SW. Indeed, the closed magnetic configuration of ICMEs (Figure 5) and the dominance of the magnetic force do not allow a significant effect of the heating magnitude on the plasma velocity inside ICMEs. It implies that the temperature of ICMEs is expected to be un-correlated with its plasma velocity, as observed.

This paper presents generic arguments to explain the almost-quadratic dependence of temperature on the velocity in the SW and the absence of dependence in ICMEs (when the entire distribution of data points is considered). These results are expected to hold for a broad range of heating mechanisms, so the observed $T(v)$ relation is not a decisive tool to test diverse heating/accelerating mechanisms of the SW. However, it does not mean that the $T(v)$ relation is independent of the heating, just that it is expected to be weakly depend on it. The analysis of this dependence will be investigated in a future work.

On the observational side, it would be important to quantify the $T(v)$ relation and test its physical origin. This cannot be done by a single spacecraft, since different plasma blobs, with different entropies, are measured. Rather it requires following the same elements of plasma with distance. This can presently be realized approximately when two spacecraft are nearly radially aligned, allowing approximately this association of plasma intervals both in the SW and in ICMEs as realized in one case by Skoug *et al.*, (2000). Having recurrent observations with at least two radially-aligned spacecraft will provide us a deep insight in the physics involved in the SW and ICMEs, and the closer these spacecraft are to the Sun the better it is since, from the above results, the $T(v)$ correlation is expected to develop close to the Sun.

Acknowledgements The author thank the anonymous referee for helpful comments.

References

Attrill, G.D.R., van Driel-Gesztelyi, L., Démoulin, P., Zhukov, A.N., Steed, K., Harra, L.K., Mandrini, C.H., Linker, J.: 2008, The Recovery of CME-Related Dimmings and the ICME's Enduring Magnetic Connection to the Sun. *Solar Phys.* **252**, 349 – 372. doi:10.1007/s11207-008-9255-z.

Cargill, P.J., Schmidt, J.M.: 2002, Modelling interplanetary CMEs using magnetohydrodynamic simulations. *Ann Geophys.* **20**, 879 – 890.

Chen, J.: 1989, Effects of toroidal forces in current loops embedded in a background plasma. *Astrophys. J.* **338**, 453 – 470.

Chen, J.: 1996, Theory of prominence eruption and propagation: Interplanetary consequences. *J. Geophys. Res.* **101**, 27499 – 27520. doi:10.1029/96JA02644.

Cranmer, S.R.: 2002, Coronal Holes and the High-Speed Solar Wind. *Space Sci. Rev.* **101**, 229 – 294.

Crooker, N.U., Horbury, T.S.: 2006, Solar Imprint on ICMEs, Their Magnetic Connectivity, and Heliospheric Evolution. *Space Sci. Rev.* **123**, 93 – 109. doi:10.1007/s11214-006-9014-0.

Démoulin, P., Dasso, S.: 2009, Causes and consequences of magnetic cloud expansion. *Astron. Astrophys.* **in press**.

Dasso, S., Mandrini, C.H., Schmieder, B., Cremades, H., Cid, C., Cerrato, Y., Saiz, E., Démoulin, P., Zhukov, A.N., Rodriguez, L., Aran, A., Menvielle, M., Poedts, S.: 2009, Linking two consecutive nonmerging magnetic clouds with their solar sources. *J. Geophys. Res.* **114**, 02109. doi:10.1029/2008JA013102.

Elliott, H.A., McComas, D.J., Schwadron, N.A., Gosling, J.T., Skoug, R.M., Gloeckler, G., Zurbuchen, T.H.: 2005, An improved expected temperature formula for identifying interplanetary coronal mass ejections. *J. Geophys. Res.* **110**, 04103. doi:10.1029/2004JA010794.

Feldman, W.C., Barraclough, B.L., Gosling, J.T., McComas, D.J., Riley, P., Goldstein, B.E., Balogh, A.: 1998, Ion energy equation for the high-speed solar wind: Ulysses observations. *J. Geophys. Res.* **103**, 14547 – 14558. doi:10.1029/98JA00963.

Gazis, P.R., Barnes, A., Mihalov, J.D., Lazarus, A.J.: 1994, Solar wind velocity and temperature in the outer heliosphere. *J. Geophys. Res.* **99**, 6561 – 6573.

Gazis, P.R., Balogh, A., Dalla, S., Decker, R., Heber, B., Horbury, T., Kilchenmann, A., Kota, J., Kucharek, H., Kunow, H., Lario, D., Potgieter, M.S., Richardson, J.D., Riley, P., Rodriguez, L., Siscoe, G., von Steiger, R.: 2006, ICMEs at High Latitudes and in the Outer Heliosphere. *Space Sci. Rev.* **123**, 417 – 451. doi:10.1007/s11214-006-9023-z.

Goldstein, B.E., Neugebauer, M., Phillips, J.L., Bame, S., Gosling, J.T., McComas, D., Wang, Y.M., Sheeley, N.R., Suess, S.T.: 1996, ULYSSES plasma parameters: latitudinal, radial, and temporal variations. *Astron. Astrophys.* **316**, 296 – 303.

Hollweg, J.V.: 1976, Collisionless electron heat conduction in the solar wind. *J. Geophys. Res.* **81**, 1649 – 1658.

Issautier, K., Meyer-Vernet, N., Moncuquet, M., Hoang, S.: 1998, Solar wind radial and latitudinal structure - Electron density and core temperature from ULYSSES thermal noise spectroscopy. *J. Geophys. Res.* **103**, 1969 – 1979.

Jian, L., Russell, C.T., Luhmann, J.G., Skoug, R.M.: 2006, Properties of Interplanetary Coronal Mass Ejections at One AU During 1995 - 2004. *Solar Phys.* **239**, 393 – 436. doi:10.1007/s11207-006-0133-2.

Leblanc, Y., Dulk, G.A., Bougeret, J.L.: 1998, Tracing the Electron Density from the Corona to 1au. *Solar Phys.* **183**, 165 – 180.

Liu, Y., Richardson, J.D., Belcher, J.W.: 2005, A statistical study of the properties of interplanetary coronal mass ejections from 0.3 to 5.4 AU. *Planet. Space Sci.* **53**, 3 – 17. doi:10.1016/j.pss.2004.09.023.

Lopez, R.E., Freeman, J.W.: 1986, Solar wind proton temperature velocity relationship. *J. Geophys. Res.* **91**, 1701 – 1705.

Maksimovic, M., Gary, S.P., Skoug, R.M.: 2000, Solar wind electron suprathermal strength and temperature gradients' Ulysses observations. *J. Geophys. Res.* **105**(A8), 18337 – 18350. doi:0148-0227/00/2000JA90003909.00.

Marsch, E., Thieme, K.M., Rosenbauer, H., Pilipp, W.G.: 1989, Cooling of solar wind electrons inside 0.3 AU. *J. Geophys. Res.* **94**, 6893 – 6898.

Matthaeus, W.H., Elliott, H.A., McComas, D.J.: 2006, Correlation of speed and temperature in the solar wind. *J. Geophys. Res.* **111**, 10103. doi:10.1029/2006JA011636.

Meyer-Vernet, N.: 2007, *Basics of solar wind*, Cambridge University Press, Cambridge.

Neugebauer, M., Steinberg, J.T., Tokar, R.L., Barraclough, B.L., Dors, E.E., Wiens, R.C., Gingerich, D.E., Luckey, D., Whiteaker, D.B.: 2003, Genesis on-board determination of the solar wind flow regime. *Space Sci. Rev.* **105**, 661 – 679. doi:10.1023/A:1024478129261.

Parker, E.N.: 1958, Dynamics of the Interplanetary Gas and Magnetic Fields. *Astrophys. J.* **128**, 664 – 676.

Parker, E.N.: 1963, *Interplanetary dynamical processes.*, Interscience Publishers, New York, 1963.

Parker, E.N.: 2007, *Solar Wind.* In: Kamide, Y., Chian, A. (eds.) *Handbook of the Solar-Terrestrial Environment*, Springer-Verlag Berlin and Heidelberg, 95 – 116.

Phillips, J.L., Feldman, W.C., Gosling, J.T., Scime, E.E.: 1995, Solar wind plasma electron parameters based on aligned observations by ICE and ULYSSES. *Adv. Space Res.* **169**, 95 – 100.

Pilipp, W.G., Miggenrieder, H., Müehlhäeuser, K.H., Rosenbauer, H., Schwenn, R.: 1990, Large-scale variations of thermal electron parameters in the solar wind between 0.3 and 1 AU. *J. Geophys. Res.* **95**, 6305 – 6329.

Richardson, J.D., Paularena, K.I., Lazarus, A.J., Belcher, J.W.: 1995, Radial evolution of the solar wind from IMP 8 to Voyager 2. *Geophys. Res. Lett.* **22**, 325 – 328.

Richardson, J.G., Cane, H.V.: 1995, Regions of abnormally low proton temperature in the solar wind and their association with ejecta. *J. Geophys. Res.* **100**, 23397.

Shen, F., Feng, X., Wu, S.T., Xiang, C.: 2007, Three-dimensional MHD simulation of CMEs in three-dimensional background solar wind with the self-consistent structure on the source surface as input: Numerical simulation of the January 1997 Sun-Earth connection event. *J. Geophys. Res.* **112**, 06109. doi:10.1029/2006JA012164.

Skoug, R.M., Feldman, W.C., Gosling, J.T., McComas, D.J., Reisenfeld, D.B., Smith, C.W., Lepping, R.P., Balogh, A.: 2000, Radial variation of solar wind electrons inside a magnetic cloud observed at 1 and 5 AU. *J. Geophys. Res.* **105**, 27269 – 27276. doi:10.1029/2000JA000095.

Totten, T.L., Freeman, J.W., Arya, S.: 1995, An empirical determination of the polytropic index for the free-streaming solar wind using HELIOS 1 data. *J. Geophys. Res.* **100**, 13 – 17.

Velli, M.: 2001, Hydrodynamics of the Solar Wind Expansion. *Astrophys. Spa. Sci.* **277**, 157 – 167. doi:10.1023/A:1012237708634.

Wang, C., Du, D., Richardson, J.D.: 2005, Characteristics of the interplanetary coronal mass ejections in the heliosphere between 0.3 and 5.4 AU. *J. Geophys. Res.* **110**, 10107. doi:10.1029/2005JA011198.

Wimmer-Schweingruber, R.F., Crooker, N.U., Balogh, A., Bothmer, V., Forsyth, R.J., Gazis, P., Gosling, J.T., Horbury, T., Kilchenmann, A., Richardson, I.G., Richardson, J.D., Riley, P., Rodriguez, L., Steiger, R.V., Wurz, P., Zurbuchen, T.H.: 2006, Understanding Interplanetary Coronal Mass Ejection Signatures. *Space Sci. Rev.* **123**, 177 – 216. doi:10.1007/s11214-006-9017-x.

Zurbuchen, T.H., Richardson, I.G.: 2006, In-Situ Solar Wind and Magnetic Field Signatures of Interplanetary Coronal Mass Ejections. *Space Sci. Rev.* **123**, 31 – 43. doi:10.1007/s11214-006-9010-4.